FTIR Studies of the Photoactivation Processes in Squid Retinochrome†

Yuji Furutani,‡,§,|| Akihisa Terakita,§,|| Yoshinori Shichida,§,|| and Hideki Kandori*,‡,||

Department of Materials Science and Engineering, Nagoya Institute of Technology, Showa-ku, Nagoya 466-8555, Japan, Department of Biophysics, Graduate School of Science, Kyoto University, Sakyo-ku, Kyoto 606-8502, Japan, and Core Research for Evolutional Science and Technology (CREST), Japan Science and Technology Corporation, Kyoto 606-8502, Japan

Received February 6, 2005; Revised Manuscript Received April 13, 2005

ABSTRACT: Retinochrome is a photoisomerase of the invertebrate visual system, which converts all-*trans*-retinal to the 11-*cis* configuration and supplies it to visual rhodopsin. In this paper, we studied light-induced structural changes in squid retinochrome by means of low-temperature UV−visible and Fourier transform infrared (FTIR) spectroscopy. In PC liposomes, lumi-retinochrome was stable in the wide temperature range between 77 and 230 K. High thermal stability of the primary intermediate in retinochrome is in contrast to the case in rhodopsins. FTIR spectroscopy suggested that the chromophore of lumi-retinochrome is in a relaxed planar 11-*cis* form, being consistent with its high thermal stability. The chromophore binding pocket of retinochrome appears to accommodate both all-*trans* and 11-*cis* forms without a large distortion, and limited protein structural changes between all-*trans* and 11-*cis* chromophores may be suitable for the function of retinochrome as a photoisomerase. The analysis of N−D and O−D stretching vibrations in D_2O revealed that the hydrogen bond of the Schiff base is weaker in retinochrome than in bovine rhodopsin and bacteriorhodopsin, while retinochrome has a water molecule under strongly hydrogen-bonded conditions (O−D stretch at 2334 cm^{-1}). The hydrogen bond of the water is further strengthened in lumi-retinochrome. The formation of meta-retinochrome accompanies deprotonation of the Schiff base, together with the peptide backbone alterations of α-helices, and possible formation of *β*-sheets. It was found that the Schiff base proton is not transferred to its counterion, Glu181, but directly released to the aqueous phase in PC liposomes (pH 7.5). This suggests that the Schiff base environment is exposed to solvent in meta-retinochrome, which may be advantageous for the hydrolysis reaction of the Schiff base in the transport of 11-*cis*-retinal to its shuttle protein.

Retinochrome is a retinal photoisomerase found in cephalopod photoreceptor cells, which is composed of seven transmembrane α-helices as in visual rhodopsins (*1*, *2*). It contains an all-*trans*-retinal via a protonated Schiff base linkage to Lys296[1] (*3*, *4*) and isomerizes selectively to the 11-*cis* configuration upon light absorption (*5*, *6*). The 11-*cis*-retinals formed in this way are supplied to visual rhodopsin molecules in an outer segment of a photoreceptor cell through a retinal-shuttle protein (*7*, *8*). Visual rhodopsin is a photosensor, and photoisomerization of the 11-*cis* chromophore to the all-*trans* form leads to protein structural changes activating a trimeric G protein. All-*trans*-retinal is released from rhodopsin by hydrolysis of the Schiff base, and then transferred to retinochrome through the retinal-shuttle protein. Thus, retinochrome has an important role as a supplier of 11-*cis*-retinal to visual rhodopsin in invertebrate vision.

The amino acid sequence of squid retinochrome is ∼20% identical to those of vertebrate and invertebrate rhodopsins (*9*). λ_{max}[2] is 495 nm, being similar to those of rhodopsins. The counterion of the protonated Schiff base in vertebrate visual rhodopsin was identified as Glu113 (*10*−*12*), whereas the corresponding amino acid is methionine in squid retinochrome. In 2000, Terakita et al. (*13*) revealed that the counterion of retinochrome is Glu181, which is located in the loop region between helices 4 and 5. The crystal structure of bovine rhodopsin was determined in the same year, and it was found that Glu181 is involved in a *β*-sheet constituting retinal binding site (*14*). Through the analysis for Go-coupled rhodopsin and peropsin from amphioxus (*Branchiostoma belcheri*), Terakita et al. (*15*) concluded that the counterion has been evolutionarily switched from position 181 to 113. Thus, retinochrome shares several similarities with rhodopsin, whereas its function is entirely different from that of rhodopsin.

† This work was supported in part by grants from Japanese Ministry of Education, Culture, Sports, Science, and Technology and by research fellowships from the Japan Society for the Promotion of Science for Young Scientists to Y.F.

* To whom correspondence should be addressed. Phone and fax: 81-52-735-5207. E-mail: kandori@nitech.ac.jp.

‡ Nagoya Institute of Technology.

§ Kyoto University.

|| Japan Science and Technology Corp.

[1] The numbers of amino acid residues described in this paper are according to the bovine rhodopsin numbering system for convenience of discussion. In the retinochrome numbering system, the number of the lysine residue is 275.

[2] Abbreviations: λ_{max}, maximum absorption wavelength; Batho, bathorhodopsin; Lumi, lumirhodopsin; Meta I, metarhodopsin I; FTIR, Fourier transform infrared; PC, L-α-phosphatidylcholine; DM, *n*-dodecyl *β*-D-maltoside; HOOP, hydrogen-out-of-plane; BR, bacteriorhodopsin; Meta II, metarhodopsin II; *pp*R, *pharaonis* phoborhodopsin (also known as *pharaonis* sensory rhodopsin II); PSB, protonated Schiff base.

10.1021/bi050219w CCC: $30.25
Published on Web 05/12/2005

Previous low-temperature UV−visible spectroscopy revealed that retinochrome solubilized by digitonin in a glycerol/water mixture is converted to prelumi-retinochrome (λ_{max} = 465 nm) (*16*), lumi-retinochrome (λ_{max} = 475 nm), and meta-retinochrome (λ_{max} = 470 nm) (*17*) in its photolytic process. Prelumi-retinochrome is stable at 25 K and thermally converted to lumi-retinochrome at 77 K (*16*) and to meta-retinochrome above 250 K (*17*). Thus, only one intermediate, lumi-retinochrome, is present in the wide temperature range from 77 to 250 K. This is in contrast to visual rhodopsins. In bovine rhodopsin, the Batho intermediate thermally converted to the Lumi intermediate above 130 K (*18*). In octopus rhodopsin, the transition temperature is 120 K (*19*). Why is lumi-retinochrome so stable in a wide temperature range? Structural changes in retinochrome have not been well understood. Only the lumi-retinochrome minus retinochrome Fourier transform infrared (FTIR) spectra were reported, showing that a protonated carboxylate changes its hydrogen-bonding condition upon retinal photoisomerization (*4*). Almost nothing is known about the structure of meta-retinochrome, though it is an important intermediate in the transfer of 11-*cis*-retinal to the shuttle protein.

In this paper, we studied the photoactivation processes of retinochrome by means of low-temperature UV−visible and FTIR spectroscopy. In PC liposomes at neutral pH, we found that lumi- and meta-retinochrome were stabilized at 77−230 and 270 K, respectively. By using site-directed mutagenesis, we assigned the protonated carboxylic group in retinochrome to Asp91, whose hydrogen bond is strengthened in lumi- and meta-retinochrome. We observed O−D stretching vibrations of water molecules which change its hydrogen bond upon formation of lumi-retinochrome. The chromophore of lumi-retinochrome is shown to be in a relaxed planar 11-*cis* form from the analysis of the HOOP modes. The planar structure of the chromophore correlates well with its thermal stability. The chromophore binding pocket of retinochrome seems to accommodate both all-*trans* and 11-*cis* forms. Formation of meta-retinochrome accompanies deprotonation of the Schiff base, together with the peptide backbone alterations of α-helices, and possible formation of β-sheets. The Schiff base proton is likely to be directly released to the aqueous phase, suggesting that the Schiff base environment is exposed to solvent in meta-retinochrome. Photoactivation processes of retinochrome are discussed on the basis of the FTIR results presented here.

MATERIALS AND METHODS

Preparation of the Wild-Type and Mutant Proteins of Retinochrome. Samples for our spectroscopic analysis were prepared as described previously (*13*). Briefly, the cDNAs of the wild-type and D91N and E181D mutant retinochromes were constructed, which were tagged by the monoclonal antibody Rho 1D4 epitope sequence (*13*). Then, the wild type and the D91N and E181D mutant proteins were expressed in HEK 293S cells, solubilized by 1% DM in HEPES buffer (pH 6.5), and purified by monoclonal antibody column chromatography.

Preparation of the Sample Film of Retinochrome. Sample preparation was described previously (*20*). Briefly, the purified retinochrome samples were reconstituted into PC liposomes (1:100 retinochrome:PC molar ratio) and dialyzed against 2 mM phosphate buffer (pH 7.5) for ∼2 weeks. Then, the sample was frozen and thawed twice and centrifuged at 15 000 rpm for 30 min at 4 °C. The pellet was resuspended in the same buffer, and the concentration was adjusted to ∼2 absorbance units (for FTIR measurements) or ∼1 absorbance unit (for UV−visible measurements) at 497 nm. A 60 μL aliquot was deposited on a BaF_2 window 18 mm in diameter and the window dried in a glass vessel that was evacuated with an aspirator. All experimental procedures were performed in dark or under dim red light (>660 nm).

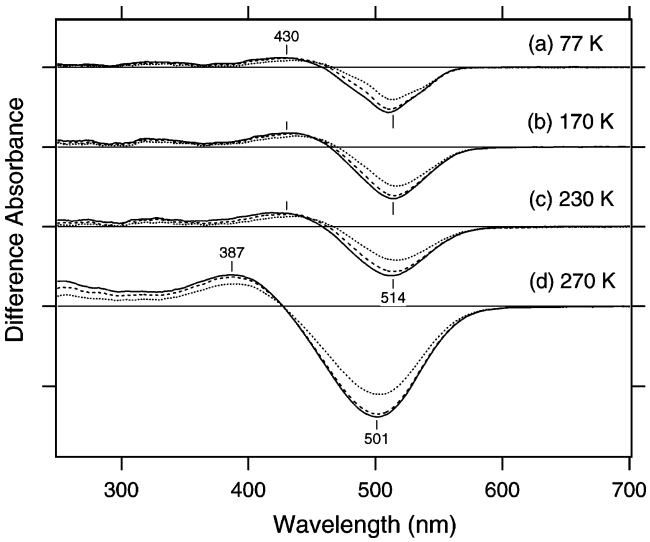

FIGURE 1: Light minus dark UV−visible difference spectra of retinochrome. Spectra were obtained at 77 (a), 170 (b), 230 (c), and 270 K (d) for hydrated films (H_2O) of squid retinochrome at pH 7.5. Irradiation was carried out with >520 nm light for 10 s (···), 1 min (- - -), and 10 min (—). Each retinochrome film has almost the same absorption at its λ_{max} (497 nm) which is slightly normalized by the factors described in the text.

UV−Visible Spectroscopy. The UV−visible spectra were measured with a UV−visible spectrometer (V-550, JASCO) equipped with a cryostat (OptistatDN, Oxford). Hydrated retinochrome films were kept at various temperatures from 77 to 270 K. Absorption spectra were recorded before and after illumination with >520 nm light for 10 s, 1 min, and 10 min, which was provided by a slide projector with a 1 kW halogen−tungsten lamp (Master HILUX-HR, Rikagaku) through an optical filter (O-54, Asahi techno glass). A fresh retinochrome film was used for the measurement at each temperature. The difference spectra shown in Figure 1 were obtained by subtracting the absorption spectra recorded in dark from those after illumination. Because each retinochrome film has different absorbance, the spectra were normalized according to the absorbance at λ_{max} (497 nm). Consequently, spectra b−d of Figure 1 were multiplied by 1.09, 1.11, and 1.05, respectively.

FTIR Spectroscopy. FTIR spectroscopy was performed as described previously (*21*). Retinochrome films were hydrated with H_2O, D_2O, or $D_2{}^{18}O$ before measurements. The sample was then placed in the cell of a cryostat (DN-1704, Oxford) mounted in an FTIR spectrometer (FTS-40, Bio-Rad). The cryostat was equipped with a temperature controller (ITC-4, Oxford), and the temperature was regulated with a precision of 0.1 K.

Illumination with >520 nm light at 77, 170, and 230 K for 1 min converted retinochrome to lumi-retinochrome. Each

difference spectrum was calculated from two spectra constructed from 128 interferograms taken before and after the illumination. Lumi-retinochrome was partially reconverted to retinochrome upon illumination with 400 nm light for 2 min, as evidenced by the difference infrared spectrum which is a mirror image with one-third intensity of that for the first retinochrome to lumi-retinochrome transition. After the first cycle of illumination, the cycles of alternating illumination with >520 and 400 nm light produced the lumi-retinochrome minus retinochrome spectra which have the same spectral shape but one-third of the intensity of the first spectrum. Sixteen difference spectra obtained in this way were averaged to produce the lumi-retinochrome minus retinochrome spectrum at each temperature.

On the other hand, illumination with >520 nm light at 270 K for 1 min converted retinochrome to meta-retinochrome. Meta-retinochrome was also partially reconverted to retinochrome upon illumination with 400 nm light. Because baseline distortion caused by the hydration change in the sample was significant at 270 K, we used a difference spectrum recorded prior to illumination as a baseline. Then, each difference spectrum was calculated from two spectra constructed from 128 interferograms taken before and after the illumination with >520 nm light, and was corrected by subtracting the baseline. Finally, the sample was illuminated with 400 nm light for 10 min to be reconverted to retinochrome for the next measurement. Eight difference spectra obtained in this way were averaged to produce the meta-retinochrome minus retinochrome spectrum.

Because linear dichroism experiments revealed the random orientation of retinochrome molecules in the liposome film, an IR polarizer was not used.

RESULTS

UV−Visible Spectroscopy. A previous study on the retinochrome sample solubilized with digitonin in a 2:1 glycerol/water mixture at pH 6.5 reported that retinochrome was converted to lumi-retinochrome (λ_{max} = 475 nm, 83 K) and stable at a wide range of temperatures from 83 to ~253 K (*17*). The study also showed that lumi-retinochrome was thermally converted to meta-retinochrome (λ_{max} = 470 nm) above 253 K. If prelumi-retinochrome (λ_{max} = 465 nm) stabilized at 25 K is included (*16*), there are only three intermediates in the photobleaching process of retinochrome. We first tested if previous observations are reproduced in the retinochrome sample reconstituted into PC liposomes.

We prepared hydrated films of the retinochrome sample in PC liposomes whose absorbances were ~0.1 at λ_{max} (497 nm). The λ_{max} was almost equal to the value reported in a previous study [495 nm (*17*)]. Each hydrated film was cooled to 77, 170, 230, or 270 K and illuminated with >520 nm light for 10 s, 1 min, and 10 min at each temperature. Figure 1a−c shows the spectra recorded at 77, 170, and 230 K, respectively. These spectra are almost identical with each other, and correspond to the lumi-retinochrome minus retinochrome difference spectra. They exhibit negative and positive peaks at 514 and 430 nm, respectively. No isosbestic point is evident as previously reported (*17*). The spectral shape is largely different at 270 K, displaying negative and positive peaks at 501 and 387 nm, respectively. A clear isosbestic point is observed at 427 nm. These results suggest

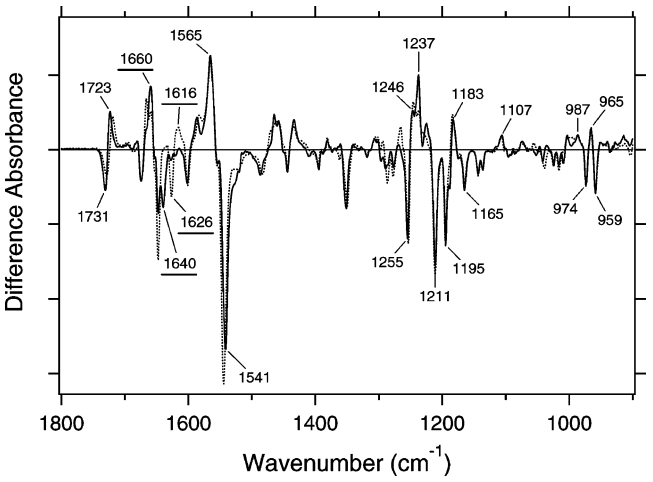

FIGURE 2: Lumi-retinochrome minus retinochrome infrared difference spectra in the 1800−900 cm^{-1} region. These spectra were measured at pH 7.5 and 77 K upon hydration with H_2O (—) and D_2O (•••). Underlined tags indicate tentatively assigned C═N stretching vibrations of the retinal Schiff base. One division of the *y*-axis corresponds to 0.002 absorbance unit.

formation of meta-retinochrome with the unprotonated Schiff base. The negative peak at 501 nm is ~3.5 times larger than the positive peak at 387 nm, probably because the molar extinction coefficient of meta-retinochrome is much smaller than that of retinochrome (~60000 cm^{-1} M^{-1}, which is ~1.5 times greater than that of rhodopsin) (*5*). From these results, we concluded that lumi-retinochrome in PC liposomes (pH 7.5) is stable below 250 K as in a glycerol/water mixture, and meta-retinochrome is formed at 270 K (*17*).

The Lumi-Retinochrome minus Retinochrome Infrared Spectra in the 1800−900 cm^{-1} Region. Sekiya et al. (*4*) reported the lumi-retinochrome minus retinochrome infrared spectra of the native squid retinochrome prepared from retinas of *Todarodes pacificus* squids. The spectra shown in Figure 2 are very similar to their spectra, indicating that the protein structure of the wild-type retinochrome expressed in cultured cells is identical to that in the native system. Similar spectra were also obtained at 170 and 230 K (data not shown).

The ethylenic C═C stretching vibrations of retinochrome and lumi-retinochrome are observed at 1541 and 1565 cm^{-1}, respectively (Figure 2). The upshift of this band upon formation of lumi-retinochrome correlates nicely with the blue shift of its absorption maximum in the UV−visible region, according to the known linear correlation between ethylenic stretch frequencies and visible absorption maxima of retinal proteins (*22*). The negative peaks at 1255, 1211, 1195, and 1165 cm^{-1} are not sensitive to H−D exchange and probably originate from the C−C stretching vibrations of retinal. These frequencies are well coincident with those of archaeal rhodopsins and protonated Schiff base of all-*trans*-retinal in solution (Table 1). Therefore, we tentatively assigned the bands at 1255, 1211, 1195, and 1165 cm^{-1} to the $C_{12}-C_{13}$, C_8-C_9, $C_{14}-C_{15}$, and $C_{10}-C_{11}$ stretching vibrations of retinochrome, respectively. Table 1 shows that the frequencies of $C_{12}-C_{13}$, C_8-C_9, and $C_{10}-C_{11}$ stretches in retinochrome are close to those of archaeal rhodopsins, whereas the $C_{14}-C_{15}$ frequency of retinochrome (1195 cm^{-1}) deviates from those of archaeal rhodopsins (1201−1204 cm^{-1}). This result suggests that the chromophore structure

Table 1: C−C Stretching Vibrations of Retinal Observed in Various Pigments

	λ_{max} (nm)	C−C stretching vibration (cm^{-1})			
		C_8-C_9	$C_{10}-C_{11}$	$C_{12}-C_{13}$	$C_{14}-C_{15}$
all-*trans* isomers					
all-*trans* PSB in solution[a]	440	1204	1159	1237	1191
retinochrome	497	1211	1165	1255	1195
pharaonis phoborhodopsin[b]	500	1213	1164	1253	1204
Neurospora rhodopsin[c]	535	1215	1166	1247	1203
bacteriorhodopsin[a]	570	1214	1170	1255	1201
11-*cis* isomers					
11-*cis* PSB in solution[d]	440	1218	1100	1237	1192
lumi-retinochrome	475	(1205)	1107	1246	1183
bovine rhodopsin[e]	500	1217	1098	1244	1190

[a] From ref *41*. [b] From refs *42* and *43*. [c] From ref *39*. [d] From ref *44*. [e] From ref *45*.

is similar in retinochrome and archaeal rhodopsins, but the Schiff base region of retinochrome is somehow different from those of archaeal rhodopsins.

Positive bands in the fingerprint region at 1246, 1183, and 1107 cm^{-1} are not sensitive to H−D exchange, while the band at 1237 cm^{-1} reduces its intensity. According to their frequencies, we also tentatively assigned the bands at 1246, 1183, and 1107 cm^{-1} to the $C_{12}-C_{13}$, $C_{14}-C_{15}$, and $C_{10}-C_{11}$ stretching vibrations of lumi-retinochrome, respectively. The C_8-C_9 stretching vibration band is possibly canceled by the intense negative bands at 1211 and 1195 cm^{-1}, because the positive band was observed at 1205 cm^{-1} in the lumi-retinochrome minus retinochrome spectrum with C_{15}-D-labeled retinal, where the negative $C_{14}-C_{15}$ stretch at 1195 cm^{-1} disappeared (*4*). The H−D sensitive positive band at 1237 cm^{-1} also disappeared in the spectrum with C_{15}-D-labeled retinal (*4*), implying that the vibration contains the vibrational mode of the Schiff base.

In the 1000−950 cm^{-1} region, corresponding to the characteristic HOOP vibrations, there are four bands at 987 (+), 974 (−), 965 (+), and 959 (−) cm^{-1}. All of them are insensitive to H−D exchange (Figure 2) and the C_{15}-D label (*4*). The negative bands at 974 and 959 cm^{-1} are also observed in the M minus BR difference spectra (data not shown), which is consistent with the fact that retinochrome has an all-*trans*-retinal. In contrast, the amplitudes of the negative bands are much greater in retinochrome. In general, intensified HOOP vibrations are interpreted in terms of chromophore distortion in the chromophore binding pocket. It is, however, unlikely that the all-*trans* chromophore has a large distortion in the unphotolyzed state whose structure is most stabilized. The C−C stretching frequencies also imply that the chromophore structure of retinochrome is similar to that in solution, a relaxed all-*trans* form (Table 1). Thus, the reason for the intensified HOOP modes should be explained in the future.

A more striking observation was that the positive HOOP bands at 987 and 965 cm^{-1} are smaller than the negative bands (Figure 2). Either band probably originates from the coupled $C_{11}H{=}C_{12}H$ HOOP mode, which is a characteristic vibrational mode of the 11-*cis* form. Bovine rhodopsin possesses a such band at 969 cm^{-1} (*23*). As described above, HOOP modes are the marker of the chromophore distortion, and intensified HOOP modes are characteristic of primary intermediates of rhodopsins. As a consequence, difference spectra of the primary intermediate minus unphotolyzed states at 77 K possess much larger positive HOOP bands for visual and archaeal rhodopsins. Smaller HOOP modes for the primary intermediate than for the unphotolyzed state are unusual, and there are presumably two reasons. One is the intensified negative bands as described above. In parallel, weak positive bands should be particularly noted. This observation suggests that lumi-retinochrome does not have a distorted chromophore structure. The presence of the relaxed planar chromophore structure is consistent with the fact that lumi-retinochrome is stable at 77−230 K (Figure 1). Thus, it seems likely that the retinal binding pocket in retinochrome accommodates not only the all-*trans* form but also the 11-*cis* form without a large distortion even at 77 K. This may help the function of retinochrome as the retinal isomerase.

A negative band at 1640 cm^{-1} in H_2O disappears in D_2O, presumably shifting to 1626 cm^{-1} (Figure 2). Sekiya et al. (*4*) observed similar bands at 1637 (+)/1626 (−) cm^{-1}, and tentatively assigned them to the C═N stretching of the retinal Schiff base. The frequency difference between the C═NH and C═ND stretching vibrations has been considered to be an indicator of hydrogen-bonding strength of the Schiff base in rhodopsins (*22*, *24*). The difference in retinochrome (14 cm^{-1}) is similar to that of BR (13 cm^{-1}) and much smaller than that for bovine rhodopsin (31 cm^{-1}). A positive band at 1660 cm^{-1} in H_2O is sensitive to H−D exchange, and a positive band is observed at 1616 cm^{-1} in D_2O (Figure 2). If these bands originate from the C═N stretching vibrations in lumi-retinochrome, the frequency difference in lumi-retinochrome (44 cm^{-1}) is larger than that in bovine rhodopsin (31 cm^{-1}), indicating that the hydrogen-bonding strength of the Schiff base becomes very strong after retinal photoisomerization. It is, however, noted that many other vibrations are contained in this frequency region, and we have shown that the hydrogen-bonding strength of the Schiff base is better characterized by the N−D stretching vibrations in D_2O, which is shown below.

Assignment of Protonated Carboxylic C═O Stretching Vibrations in the Lumi-Retinochrome minus Retinochrome Spectrum. The frequency region between 1800 and 1580 cm^{-1} in Figure 2 is expanded in Figure 3a. The bands at 1731 (−) and 1723 (+) cm^{-1} are downshifted to 1729 (−) and 1720 (+) cm^{-1}, respectively, upon hydration with D_2O. They are likely to originate from C═O stretching vibrations of a protonated carboxylic group. In fact, these bands completely disappear in the spectra of the D91N mutant (λ_{max} = 490 nm), while new bands appeared at 1704 (−) and 1695 (+) cm^{-1} (Figure 3b). These frequencies are characteristic of the C═O stretching vibrations of asparagines, and the H−D unexchangeable nature of the bands (Figure 3b) is also consistent with the assignment. We thus concluded that Asp91 is protonated in retinochrome and the hydrogen bond is strengthened upon formation of lumi-retinochrome. These results are also consistent with the previous conclusion that Glu181 acts as the counterion of the Schiff base in retinochrome (*13*), because there are no signals in the 1800−1700 cm^{-1} region (Figure 3). Glu181 is presumably deprotonated.

O−D Stretching Vibrations of Water Molecules under Strongly Hydrogen-Bonding Conditions. We first reported the difference spectra of BR in the X−D (X = N or O) stretching vibrations (2700−2000 cm^{-1}) in D_2O, which can

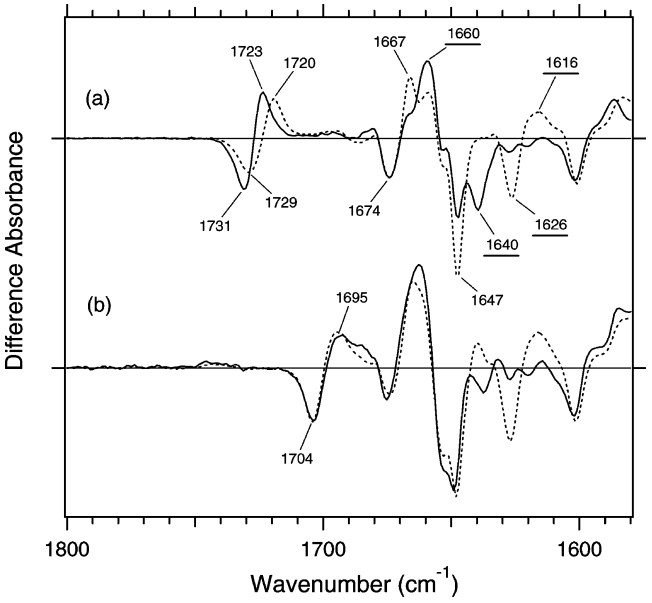

FIGURE 3: Lumi-retinochrome minus retinochrome infrared difference spectra in the 1800−1580 cm^{-1} region. The spectra in panel a were reproduced from Figure 2. In panel b, the spectra depicted as solid and dotted lines were obtained by assessing the retinochrome D91N mutant hydrated with H_2O and D_2O, respectively. One division of the *y*-axis corresponds to 0.005 absorbance unit.

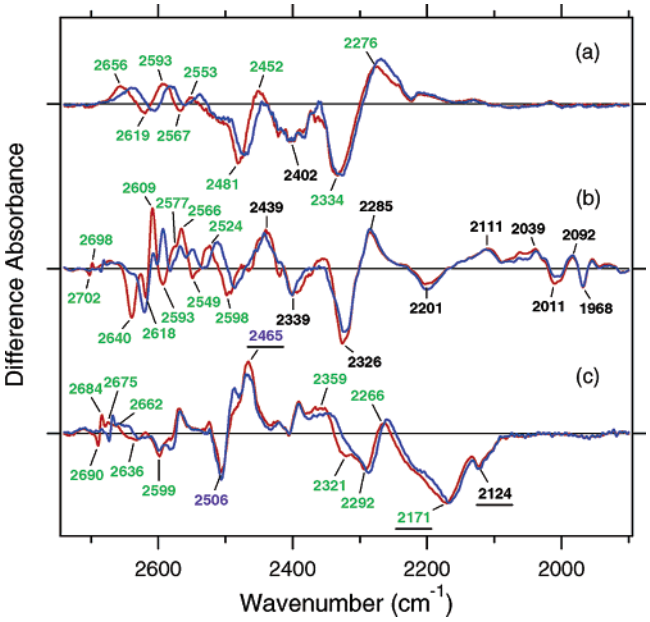

FIGURE 4: Comparison of the lumi-retinochrome minus retinochrome (a), Batho minus rhodopsin (b), and K minus BR (c) difference infrared spectra in the 2730−1950 cm^{-1} region. These spectra were measured at 77 K after the samples had been hydrated with D_2O (red lines) and $D_2{}^{18}O$ (blue lines). Frequencies labeled in green correspond to those identified as water stretching vibrations. Frequencies labeled in purple are O−D stretches of Thr89 (*46*, *47*), while the underlined frequencies are N−D stretches of the Schiff base (*29*). Spectra in panels b and c were reproduced from Tanimoto et al. (*28*) and Furutani et al. (*21*), respectively. One division of the *y*-axis corresponds to 0.001 absorbance unit.

monitor hydrogen-bonding alterations of H−D exchangeable vibrations in protein and internal water molecules (*25*). On the basis of such measurements, we found the presence of strongly hydrogen-bonded water molecules in BR, whose O−D stretching vibrations appear at <2400 cm^{-1} (*26*). In the K minus BR difference spectra at 77 K (Figure 4c), the bands at 2359 (+), 2321 (−), 2292 (−), 2266 (+), and 2171 (−) cm^{-1} originate from such water molecules because of the isotope shift of $D_2{}^{18}O$. Recently, we identified the O−D stretch at 2171 cm^{-1} as the bridged water molecule between the protonated Schiff base and its counterion (Asp85) (*27*). Hydrogen-bonding alteration of the water molecule plays an important role in the proton transfer reaction from the Schiff base to Asp85 (*28*). In contrast to BR, no water bands were detected for vertebrate visual rhodopsin (Batho minus bovine rhodopsin spectra) at 77 K as shown in Figure 4b. In case of bovine rhodopsin, no water bands below 2400 cm^{-1} are observed for the difference spectra of Lumi, Meta I, and Meta II intermediates. We thus concluded that strongly hydrogen-bonded water molecules do not play important roles in the photoactivation processes of bovine rhodopsin (*21*). In this way, difference infrared spectra at <2400 cm^{-1} provide fruitful information about the water-containing hydrogen-bonding network inside the protein.

The lumi-retinochrome minus retinochrome spectrum in Figure 4a clearly shows the presence of water bands at 2334 (−) and 2276 (+) cm^{-1} in the <2400 cm^{-1} region. These bands downshift to 2326 (−) and 2269 (+) cm^{-1}, respectively, upon hydration with $D_2{}^{18}O$, exhibiting the 7−8 cm^{-1} isotope shift. It is noted that the isotope shift of water is smaller than those in the higher-frequency region (2660−2450 cm^{-1}), suggesting that other vibrations may be involved at 2334 (−) and 2276 (+) cm^{-1}. In fact, similar bands were observed at 2326 (−) and 2285 (+) cm^{-1} in bovine rhodopsin that do not originate from water O−D stretches (Figure 4b). They may originate from H−D exchangeable amide A vibrations (N−D stretches of the peptide backbone). Because structural changes in retinochrome are limited around the chromophore at 77 K, such water molecules in Figure 4a must be present near the retinal. We infer that the water molecule(s) hydrates negative charges near the retinal chromophore. Glu181 is likely to be the hydrogen-bonding acceptor of the water, because it has a negative charge as the counterion of the Schiff base (*13*).

The bands at 2656 (+), 2619 (−), 2593 (+), 2567 (−), 2553 (+), 2481 (−), and 2452 (+) cm^{-1} are also assigned to O−D stretching vibrations of water molecules. One of them could correspond to another O−D stretch of the 2334 cm^{-1} band in the water molecule hydrating to Glu181. In total, four negative bands could be assigned to the water O−D stretching (Figure 4a), which is considerably smaller in number than those of rhodopsin and BR. This fact suggests that there are fewer internal water molecules around the retinal chromophore in retinochrome. Another interesting issue is that water bands of retinochrome in the 2700−2500 cm^{-1} region are significantly broadened (Figure 4a). In this frequency region, water bands are generally sharp because of weak hydrogen bonds, which is typically shown for rhodopsin and BR (spectra b and c of Figure 4). This may suggest that water molecules are not positionally fixed in retinochrome compared with those in rhodopsin and BR.

N−D Stretching Vibrations of the Retinal Schiff Base. The N−D stretching vibrations of the Schiff base have been assigned in BR and *pp*R to 2171 and 2124 cm^{-1} (Figure 4c) and 2140 and 2091 cm^{-1}, respectively, by use of a [^{15}N]-Lys-labeled protein (*29*, *30*). After retinal photoisomerization, the N−D stretches of the K intermediate appear at 2465 cm^{-1}

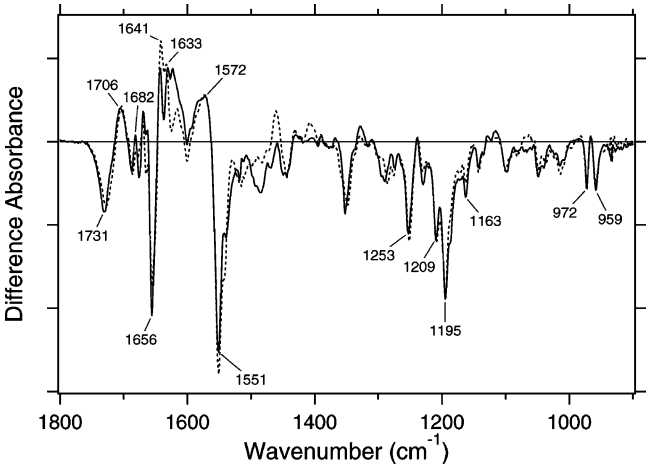

FIGURE 5: Meta-retinochrome minus retinochrome infrared difference spectra in the 1800−900 cm^{-1} region. These spectra were measured at pH 7.5 and 270 K upon hydration with H_2O (−) and D_2O (•••). One division of the *y*-axis corresponds to 0.002 absorbance unit.

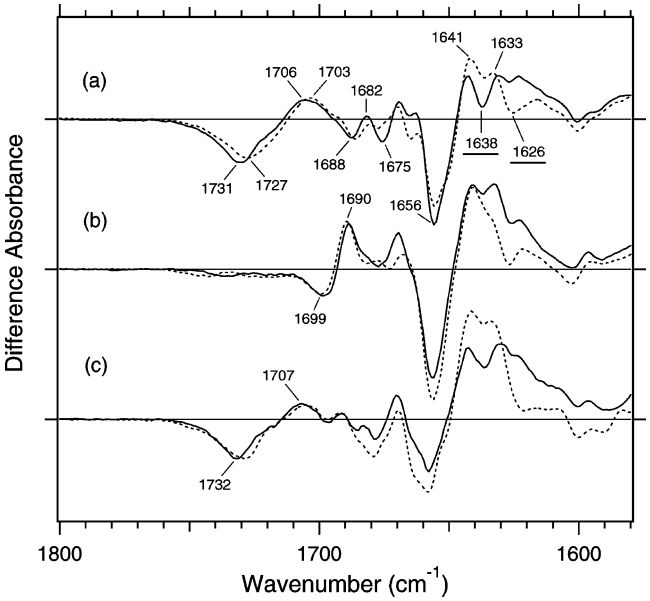

FIGURE 6: Meta-retinochrome minus retinochrome infrared difference spectra in the 1800−1580 cm^{-1} region. The spectra in panel a were reproduced from Figure 5. The spectra in panels b and c were obtained by assessing retinochrome D91N and E181D mutants, respectively. The solid and dotted lines indicate that the samples are hydrated with H_2O and D_2O, respectively. One division of the *y*-axis corresponds to 0.006 absorbance unit.

(Figure 4c) and 2474 cm^{-1} for BR and *p*pR, respectively, indicating that the hydrogen bond of the Schiff base is significantly weakened because of the rotation of the N−D group. Although the N−D stretch of the Schiff base has not been assigned for bovine rhodopsin by use of [^{15}N]Lys labeling, previous analysis suggested that the N−D stretch of rhodopsin is present at ∼2000 cm^{-1} (*21*). The spectral feature in Figure 4b at ∼2000 cm^{-1} implies that Batho also has the N−D stretch at the same frequency region.

In the case of retinochrome, there are no bands in the 2200−1900 cm^{-1} region (Figure 4a), where N−D stretches of rhodopsin and BR are present. This spectral feature is not limited to 77 K, but is also observed at 170 and 230 K (data not shown). Thus, N−D stretching of retinochrome may be assigned to 2402 or 2334 cm^{-1}, though the latter was assigned to water O−D stretching. Interestingly, the analysis of the C═N stretching vibrations suggests that the hydrogen-bonding strength of the Schiff base is similar for retinochrome and BR, since the frequency differences between the C═NH and C═ND stretching vibrations are 14 and 13 cm^{-1} for retinochrome and BR, respectively. According to a more direct measurement of the hydrogen-bonding strength of the Schiff base (N−D stretch in D_2O), however, it is likely that the hydrogen bond of the Schiff base in retinochrome is weaker than that in BR.

Meta-Retinochrome minus Retinochrome Infrared Spectra in the 1800−900 cm^{-1} Region. Above 250 K, retinochrome is photoconverted to meta-retinochrome, from which 11-*cis*-retinal is transferred to a retinal-shuttle protein. Sekiya et al. (*4*) reported the meta-retinochrome minus retinochrome spectra only in the protonated carboxylic C═O stretching vibrations (1800−1700 cm^{-1}). Figure 5 shows the meta-retinochrome minus retinochrome spectra in the 1800−900 cm^{-1} region. The negative bands at 1253, 1209, 1195, and 1163 cm^{-1} correspond to the C−C stretching vibrations of retinochrome as seen in Figure 2. The negative bands at 972 and 959 cm^{-1} are HOOP vibrations of retinochrome. The large negative peak at 1551 cm^{-1} corresponds to the C═C stretching vibration of retinochrome. On the positive side, there are almost no bands below 1500 cm^{-1}. This suggests that the Schiff base of the retinal chromophore in meta-retinochrome is deprotonated under the present condition (PC liposomes at pH 7.5), because the chromophore vibrations are known to reduce the IR intensities when the Schiff base loses a positive charge. This observation is consistent with the λ_{max} of meta-retinochrome at 387 nm (Figure 1d).

In contrast to the <1500 cm^{-1} region, large bands are observed in the amide I region (Figures 5 and 6a). Tagged bands in Figure 6a at 1638 and 1626 cm^{-1} in H_2O and D_2O, respectively, resemble to those at 1640 and 1626 cm^{-1}, respectively, in the lumi-retinochrome minus retinochrome spectra (Figure 3a), which can be ascribed to the C═N stretching vibrations of the Schiff base in retinochrome. The bands at 1656 (−), 1641 (+), and 1633 (+) cm^{-1} are not sensitive to the H−D exchange, suggesting that they originate from amide I modes embedded in the membrane. The negative frequency at 1656 cm^{-1} is characteristic of the amide I vibration of the α-helix. This band is upshifted in lumi-retinochrome (Figure 3a), but downshifted in meta-retinochrome (Figure 6a). This implies that hydrogen bonds of α-helices are weakened in lumi-retinochrome, while being strengthened in meta-retinochrome. The appearance of the positive bands in the 1640−1620 cm^{-1} region may also suggest formation of *β*-sheet, which could be formed from helical structures.

Assignment of Protonated Carboxylic C═O Stretching Vibrations in the Meta-Retinochrome minus Retinochrome Spectrum. In the meta-retinochrome minus retinochrome spectra (Figure 6a), the bands at 1731 (−) and 1706 (+) cm^{-1} are downshifted to 1727 (−) and 1703 (+) cm^{-1}, respectively, upon hydration with D_2O, like the 1731 (−) and 1723 (+) cm^{-1} bands in the lumi-retinochrome minus retinochrome spectra (Figure 3a). This fact suggests that they originate from the C═O stretching vibrations of Asp91. Indeed, these bands disappear in the spectra of the D91N mutant, while new bands appeared at 1699 (−) and 1690

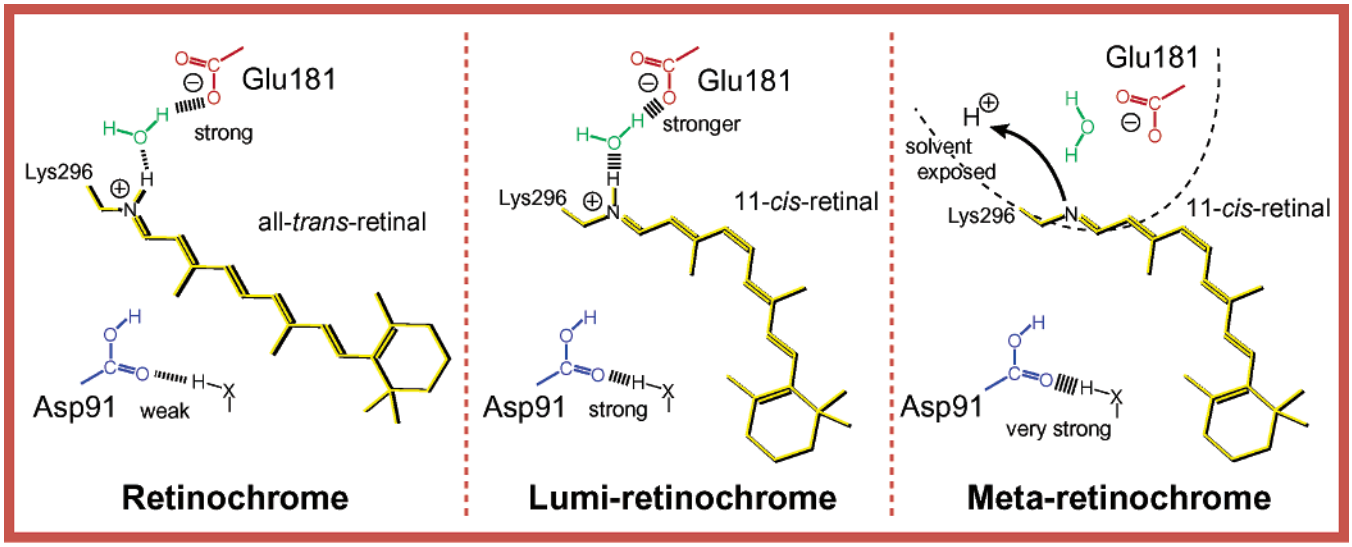

FIGURE 7: Structural changes upon retinal photoisomerization in retinochrome. The hydrogen-bonding strength of Asp91 becomes strong in lumi-retinochrome, while being further strengthened in meta-retinochrome. The Schiff base deprotonation occurs upon formation of the the meta-retinochrome, probably because the region is exposed to solvent. Glu181 works as a counterion of the Schiff base and is always deprotonated.

(+) cm^{-1} (Figure 6b). Thus, the C═O stretch of protonated Asp91 is at 1731 cm^{-1} in retinochrome, while it is at 1723 and 1706 cm^{-1} in lumi-retinochrome and meta-retinochrome, respectively. Its hydrogen bond is strengthened during the photoactivation processes of retinochrome. It should be noted that the frequency at 1706 cm^{-1} in meta-retinochrome is very low for the C═O stretching of protonated aspartic acids, suggesting a very specific environment around Asp91 in meta-retinochrome.

Figure 6c shows the meta-retinochrome minus retinochrome spectra of the E181D mutant protein (λ_{max} = 501 nm). The spectral feature of the 1750−1700 cm^{-1} region is identical between the wild type and E181D (spectra a and c of Figure 6), indicating that the vibrational bands of Asp91 are not affected by the structural modification between glutamate and aspartate at position 181. Thus, Asp91 is probably located in the position that is not connected to Glu181 through the hydrogen-bonding network.

The mutation analysis shown in Figure 6 also provided important information about the mechanism of pK_a control in meta-retinochrome. Glu181 is the counterion of the protonated Schiff base in retinochrome (*13*). Therefore, we expected that the Schiff base proton is probably transferred to Glu181 upon formation of meta-retinochrome (λ_{max} = 387 nm; Figure 1). In bovine rhodopsin, the counterion Glu113 is the proton acceptor of the Schiff base upon formation of Meta II (*31*). Nevertheless, Figure 6 shows that the vibrational bands in the 1750−1700 cm^{-1} region originate from only Asp91, and no protonation signal of Glu181 was observed. This result excluded the possibility of carboxylates as the proton acceptor of the Schiff base in meta-retinochrome. At present, there are two possible mechanisms of proton transfer from the Schiff base. In one, the proton acceptor is present inside the protein, whose candidate is either an amino acid side chain or a water molecule. In another, the proton is released from the Schiff base to an aqueous phase. Previous study suggested that the photobleaching process of retinochrome is faster at pH 6.3 than at pH 5.6 (*32*). We thus infer that the deprotonation of the Schiff base in meta-retinochrome is caused not by an internal proton transfer reaction but by the solvent-exposed environment.

DISCUSSION

In this paper, we studied structural changes accompanying photoactivation processes of squid retinochrome by means of low-temperature UV−visible and FTIR spectroscopy. Two intermediates, lumi-retinochrome and meta-retinochrome, were observed in membranes (PC liposomes) like in a digitonin detergent (*17*). We found that lumi-retinochrome is more stable (77−230 K) than the primary intermediates of rhodopsins. FTIR spectroscopy suggested that the chromophore of lumi-retinochrome is in a relaxed planar 11-*cis* form. The formation of meta-retinochrome accompanies deprotonation of the Schiff base, whereas the Schiff base proton is not transferred to its counterion, Glu181. The proton is likely to be released to the aqueous phase in PC liposomes (pH 7.5), suggesting that the Schiff base environment is exposed to solvent in meta-retinochrome. Retinochrome is composed of seven-transmembrane helices such as bovine rhodopsin, but its structure is unknown. These results provided fruitful information about the structure of retinochrome and structural changes for its photoactivation. Here we present a schematic model of the photoactivation processes of retinochrome on the basis of our FTIR observations (Figure 7).

Structure of Retinochrome. The counterion of the Schiff base in retinochrome was identified as Glu181 (*13*). In bovine rhodopsin, Glu181 is located in the loop region between helices 4 and 5, and the region constitutes antiparallel β-sheet structure (*14*). From the hydropathy plot of retinochrome, Glu181 is presumably located in the loop region, though it is not clear if the region forms β-sheets. Thus, it seems likely that the extracellular loop region constitutes the retinal binding pocket in rhodopsin and retinochrome. Glu181 acts as a counterion of the Schiff base in an invertebrate rhodopsin, Go-coupled rhodopsin, and peropsin from amphioxus (*B. belcheri*) (*15*). An important role of the amino

acid at position 181 in color tuning has been also reported for long-wavelength visual pigments (iodopsin and human red) and VA opsins. A chloride ion is bound to histidine at position 181 (*33*), for which the λ_{max} is shifted to red by ~40 nm (*34*−*36*). This FTIR study supports the idea that Glu181 is deprotonated in retinochrome, by which it works as the counterion of the Schiff base.

Asp91 is the only carboxylic acid in a transmembrane region of retinochrome. Therefore, Asp91 has been considered to be one candidate for the Schiff base counterion in retinochrome. However, our FTIR study clearly showed that the side chain of Asp91 is in a protonated form, which excluded the possibility of the Schiff base counterion. In addition, this FTIR study provided more detailed information about the microenvironment of Asp91. The hydrogen bond of Asp91 is altered in the photoconversion of retinochrome to lumi-retinochrome at 77 K, suggesting that Asp91 is located near the retinal chromophore. The C═O stretching frequency at 1731 cm^{-1} indicates that Asp91 forms a hydrogen bond (Figure 3). Nevertheless, the hydrogen-bonding network is not linked to that of Glu181 (Figure 7), because the C═O stretch of Asp91 is not affected by the mutation of Glu181 to Asp (Figure 6).

There is a water molecule under strongly hydrogen-bonded conditions (O−D stretch at 2334 cm^{-1}; Figure 4a). This water is probably located near the chromophore of retinochrome, because its frequency change was observed under the frozen conditions at 77 K. In Figure 7, we propose that the negatively charged Glu181 is the hydrogen-bonding acceptor of the water. Other water molecules shown in Figure 4a are presumably located near the retinal chromophore depending on their hydrogen-bonding strengths (weak at 2619 and 2567 cm^{-1} and moderate at 2481 cm^{-1}).

The hydrogen-bonding strength of the Schiff base in retinochrome is complicated. It is likely that the C═N stretch is at 1640 cm^{-1} in H_2O and at 1626 cm^{-1} in D_2O (Figure 3a). The frequency difference (14 cm^{-1}) is similar to that of BR (13 cm^{-1}), suggesting that the hydrogen-bonding strength of the Schiff base is similar between retinochrome and BR. However, no bands were observed at ~2171 and ~2124 cm^{-1} (Figure 4a), where the N−D stretching vibration of BR appears (Figure 4c). From the analysis of the N−D stretch, we conclude that the hydrogen bond of the Schiff base is weaker in retinochrome than in BR. It is plausible because the N−D stretch is a more direct probe of the hydrogen-bonding strength of the Schiff base than the analysis by C═NH and C═ND stretches. In our model of retinochrome (Figure 7), we place a water molecule between the Schiff base and Glu181 as is the case for BR, whereas the hydrogen bond of the Schiff base with the water is weak in retinochrome.

C−C stretching vibrations of the retinal chromophore indicate that the chromophore structure is similar between retinochrome and archaeal rhodopsins, whereas the Schiff base region of retinochrome is somehow different from those of archaeal rhodopsins. The latter may originate from the different hydrogen-bonding environment. Another interesting issue is the C_6−C_7 conformation in retinochrome. The single bond is in a *trans* form in archaeal rhodopsins, which contributes a spectral red shift because of extended conjugated double bonds (*37*). In contrast, it is in a *cis* form in visual rhodopsins (*38*). Although our study does not provide direct experimental proof, we infer that the C_6−C_7 conformation is in a *cis* form in retinochrome because the hydrogen bond of the Schiff base is very weak, and the polyene chain is similar to those of archaeal rhodopsins. Therefore, it is likely that the λ_{max} at 497 nm is better explained by the C_6−C_7 *cis* form like in visual rhodopsins (Figure 7).

Structure of Lumi-Retinochrome. Lumi-retinochrome has two unique characteristics that are in contrast to those of primary intermediates in rhodopsins: color and thermal stability. Lumi is blue-shifted, whereas most primary photointermediates of rhodopsins are red-shifted. In archaeal rhodopsins, the protonated Schiff base significantly weakens the hydrogen bond, which is one of major factors of its red shift (*29*, *30*, *39*). In visual rhodopsins, the hydrogen bond of the Schiff base is unaltered, while the middle of the polyene chain is highly twisted (*40*). Since the hydrogen bond of the Schiff base is weak in retinochrome, a strengthened hydrogen bond may contribute the color change. Formation of the strong hydrogen bond of a water molecule (Figure 4a) possibly contributes to the strong interaction of the Schiff base with its counterion, Glu181 (Figure 7).

Weak HOOP modes (Figure 2) strongly suggest that lumi-retinochrome does not have a distorted chromophore structure. The relaxed planar chromophore structure is consistent with the fact that lumi-retinochrome is stable at 77−230 K (Figure 1). Thus, it seems likely that the retinal binding pocket in retinochrome accommodates not only the all-*trans* form but also the 11-*cis* form without a large distortion even at 77 K. This may favor the function of retinochrome as the retinal isomerase. In other words, it is not necessary for retinochrome to change the protein structure significantly, whereas rhodopsin has to do it for intramolecular signal transduction from the chromophore-binding extracellular domain to the cytoplasmic surface.

Structure of Meta-Retinochrome. Previous UV−visible spectroscopy reported the λ_{max} of meta-retinochrome at 470 nm, suggesting that the Schiff base is protonated (*17*). The measurement was carried out for the retinochrome sample in a digitonin solution with a 2:1 glycerol/water mixture at pH 6.5. In our study, meta-retinochrome probably has a deprotonated Schiff base, because it possesses a λ_{max} of 380 nm (Figure 1). The absence of positive bands in the 1400−900 cm^{-1} region of meta-retinochrome minus retinochrome spectra also supports such deprotonation (Figure 5). We prepared the retinochrome sample in PC liposomes at pH 7.5, and different λ_{max} values can be explained by differences in sample preparation. In fact, a previous study showed that the UV−visible spectra in the absence of glycerol exhibit two peaks near 380 and 470 nm, which correspond to meta-retinochrome with deprotonated and protonated Schiff bases, respectively (*17*). It seems that glycerol increases the pK_a of the Schiff base in meta-retinochrome.

It seems likely that the pK_a of the Schiff base in meta-retinochrome depends on sample conditions. Although we did not measure the pK_a value in PC liposomes, it should be <7. Thus, formation of meta-retinochrome in a membrane under physiological conditions probably accompanies deprotonation of the Schiff base. A significant drop in the pK_a from the unphotolyzed to the active state is common between bovine rhodopsin and squid retinochrome. However, the mechanism is far different between them. In bovine rhodopsin, the proton transfer takes place from the Schiff base to

its counterion, and FTIR spectroscopy detected a protonation signal of Glu113 in Meta II (*31*). In contrast, our FTIR study of squid retinochrome could not detect any protonation signals of carboxylates even after deprotonation of the Schiff base (Figure 6). This fact strongly suggests that the Schiff base proton is released directly to the aqueous phase. For such an event, the Schiff base environment will be exposed to solvent. It is noted that the function of retinochrome is not only to isomerize the all-*trans*-retinal to the 11-*cis* form. After photoconversion of the all-*trans* form to the 11-*cis* form, the Schiff base linkage has to be broken to transfer the retinal to the soluble shuttle protein. The solvent-exposed environment of the Schiff base in meta-retinochrome probably favors the hydrolysis reaction.

ACKNOWLEDGMENT

We thank Kana Okada of Kyoto University for her help in preparing retinochrome.

REFERENCES

1. Hara, T., and Hara, R. (1965) New photosensitive pigment found in the retina of the squid *Ommastrephes*, *Nature 206*, 1331−1334.
2. Hara, T., and Hara, R. (1967) Rhodopsin and retinochrome in the squid retina, *Nature 214*, 573−575.
3. Hara-Nishimura, I., Kondo, M., Nishimura, M., Hara, R., and Hara, T. (1993) Amino acid sequence surrounding the retinal-binding site in retinochrome of the squid, *Todarodes pacificus*, *FEBS Lett. 335*, 94−98.
4. Sekiya, N., Kishigami, A., Naoki, H., Chang, C. W., Yoshihara, K., Hara, R., Hara, T., and Tokunaga, F. (1991) Fourier transform infrared spectroscopic study on retinochrome and its primary photoproduct, lumiretinochrome, *FEBS Lett. 280*, 107−111.
5. Hara, T., and Hara, R. (1973) Isomerization of retinal catalysed by retinochrome in the light, *Nat. New Biol. 242*, 39−43.
6. Hara, T., and Hara, R. (1968) Regeneration of squid retinochrome, *Nature 219*, 450−454.
7. Ozaki, K., Terakita, A., Hara, R., and Hara, T. (1987) Isolation and characterization of a retinal-binding protein from the squid retina, *Vision Res. 27*, 1057−1070.
8. Terakita, A., Hara, R., and Hara, T. (1989) Retinal-binding protein as a shuttle for retinal in the rhodopsin-retinochrome system of the squid visual cells, *Vision Res. 29*, 639−652.
9. Hara-Nishimura, I., Matsumoto, T., Mori, H., Nishimura, M., Hara, R., and Hara, T. (1990) Cloning and nucleotide sequence of cDNA for retinochrome, retinal photoisomerase from the squid retina, *FEBS Lett. 271*, 106−110.
10. Nathans, J. (1990) Determinants of visual pigment absorbance: Identification of the retinylidene Schiff's base counterion in bovine rhodopsin, *Biochemistry 29*, 9746−9752.
11. Sakmar, T. P., Franke, R. R., and Khorana, H. G. (1989) Glutamic acid-113 serves as the retinylidene Schiff base counterion in bovine rhodopsin, *Proc. Natl. Acad. Sci. U.S.A. 86*, 8309−8313.
12. Zhukovsky, E. A., and Oprian, D. D. (1989) Effect of carboxylic acid side chains on the absorption maximum of visual pigments, *Science 246*, 928−930.
13. Terakita, A., Yamashita, T., and Shichida, Y. (2000) Highly conserved glutamic acid in the extracellular IV−V loop in rhodopsins acts as the counterion in retinochrome, a member of the rhodopsin family, *Proc. Natl. Acad. Sci. U.S.A. 97*, 14263−14267.
14. Palczewski, K., Kumasaka, T., Hori, T., Behnke, C. A., Motoshima, H., Fox, B. A., Le Trong, I., Teller, D. C., Okada, T., Stenkamp, R. E., Yamamoto, M., and Miyano, M. (2000) Crystal structure of rhodopsin: A G protein-coupled receptor, *Science 289*, 739−745.
15. Terakita, A., Koyanagi, M., Tsukamoto, H., Yamashita, T., Miyata, T., and Shichida, Y. (2004) Counterion displacement in the molecular evolution of the rhodopsin family, *Nat. Struct. Mol. Biol. 11*, 284−289.
16. Tokunaga, F., Watanabe, T., Uematsu, J., Hara, R., and Hara, T. (1990) Photoreactions of retinochrome at very low temperatures, *FEBS Lett. 262*, 266−268.
17. Hara, R., Hara, T., Tokunaga, F., and Yoshizawa, T. (1981) Photochemistry of retinochrome, *Photochem. Photobiol. 33*, 883−891.
18. Maeda, A., Ohkita, Y. J., Sasaki, J., Shichida, Y., and Yoshizawa, T. (1993) Water structural changes in lumirhodopsin, metarhodopsin I, and metarhodopsin II upon photolysis of bovine rhodopsin: Analysis by Fourier transform infrared spectroscopy, *Biochemistry 32*, 12033−12038.
19. Nishimura, S., Kandori, H., Nakagawa, M., Tsuda, M., and Maeda, A. (1997) Structural dynamics of water and the peptide backbone around the Schiff base associated with the light-activated process of octopus rhodopsin, *Biochemistry 36*, 864−870.
20. Nagata, T., Terakita, A., Kandori, H., Kojima, D., Shichida, Y., and Maeda, A. (1997) Water and peptide backbone structure in the active center of bovine rhodopsin, *Biochemistry 36*, 6164−6170.
21. Furutani, Y., Shichida, Y., and Kandori, H. (2003) Structural changes of water molecules during the photoactivation processes in bovine rhodopsin, *Biochemistry 42*, 9619−9625.
22. Aton, B., Doukas, A. G., Callender, R. H., Becher, B., and Ebrey, T. G. (1977) Resonance Raman studies of the purple membrane, *Biochemistry 16*, 2995−2999.
23. Eyring, G., Curry, B., Broek, A., Lugtenburg, J., and Mathies, R. (1982) Assignment and interpretation of hydrogen out-of-plane vibrations in the resonance Raman spectra of rhodopsin and bathorhodopsin, *Biochemistry 21*, 384−393.
24. Baasov, T., Friedman, N., and Sheves, M. (1987) Factors affecting the C═N stretching in protonated retinal Schiff base: A model study for bacteriorhodopsin and visual pigments, *Biochemistry 26*, 3210−3217.
25. Kandori, H., Kinoshita, N., Shichida, Y., and Maeda, A. (1998) Protein Structural Changes in Bacteriorhodopsin upon Photoisomerization As Revealed by Polarized FTIR Spectroscopy, *J. Phys. Chem. B 102*, 7899−7905.
26. Kandori, H., and Shichida, Y. (2000) Direct Observation of the Bridged Water Stretching Vibrations Inside a Protein, *J. Am. Chem. Soc. 122*, 11745−11746.
27. Shibata, M., Tanimoto, T., and Kandori, H. (2003) Water Molecules in the Schiff Base Region of Bacteriorhodopsin, *J. Am. Chem. Soc. 125*, 13312−13313.
28. Tanimoto, T., Furutani, Y., and Kandori, H. (2003) Structural changes of water in the Schiff base region of bacteriorhodopsin: Proposal of a hydration switch model, *Biochemistry 42*, 2300−2306.
29. Kandori, H., Belenky, M., and Herzfeld, J. (2002) Vibrational frequency and dipolar orientation of the protonated Schiff base in bacteriorhodopsin before and after photoisomerization, *Biochemistry 41*, 6026−6031.
30. Shimono, K., Furutani, Y., Kamo, N., and Kandori, H. (2003) Vibrational modes of the protonated Schiff base in *pharaonis* phoborhodopsin, *Biochemistry 42*, 7801−7806.
31. Jager, F., Fahmy, K., Sakmar, T. P., and Siebert, F. (1994) Identification of glutamic acid 113 as the Schiff base proton acceptor in the metarhodopsin II photointermediate of rhodopsin, *Biochemistry 33*, 10878−10882.
32. Ozaki, K., Hara, R., and Hara, T. (1982) Dependency of absorption characteristics of retinochrome on pH and salts, *Exp. Eye Res. 34*, 499−508.
33. Wang, Z., Asenjo, A. B., and Oprian, D. D. (1993) Identification of the Cl^--binding site in the human red and green color vision pigments, *Biochemistry 32*, 2125−2130.
34. Shichida, Y., Kato, T., Sasayama, S., Fukada, Y., and Yoshizawa, T. (1990) Effects of chloride on chicken iodopsin and the chromophore transfer reactions from iodopsin to scotopsin and B-photopsin, *Biochemistry 29*, 5843−5848.
35. Knowles, A. (1980) The chloride effect in chicken red cone receptors, *Vision Res. 20*, 475−483.
36. Fager, L. Y., and Fager, R. S. (1979) Halide control of color of the chicken cone pigment iodopsin, *Exp. Eye Res. 29*, 401−408.
37. Harbison, G. S., Smith, S. O., Pardoen, J. A., Courtin, J. M., Lugtenburg, J., Herzfeld, J., Mathies, R. A., and Griffin, R. G. (1985) Solid-state ^{13}C NMR detection of a perturbed 6-s-trans chromophore in bacteriorhodopsin, *Biochemistry 24*, 6955−6962.
38. Mollevanger, L. C., Kentgens, A. P., Pardoen, J. A., Courtin, J. M., Veeman, W. S., Lugtenburg, J., and de Grip, W. J. (1987) High-resolution solid-state ^{13}C NMR study of carbons C-5 and C-12 of the chromophore of bovine rhodopsin. Evidence for a 6-S-cis conformation with negative-charge perturbation near C-12, *Eur. J. Biochem. 163*, 9−14.

39. Furutani, Y., Bezerra, A. G., Jr., Waschuk, S., Sumii, M., Brown, L. S., and Kandori, H. (2004) FTIR Spectroscopy of the K Photointermediate of *Neurospora* Rhodopsin: Structural Changes of the Retinal, Protein, and Water Molecules after Photoisomerization, *Biochemistry 43*, 9636−9646.
40. Palings, I., van den Berg, E. M., Lugtenburg, J., and Mathies, R. A. (1989) Complete assignment of the hydrogen out-of-plane wagging vibrations of bathorhodopsin: Chromophore structure and energy storage in the primary photoproduct of vision, *Biochemistry 28*, 1498−1507.
41. Smith, S. O., Myers, A. B., Mathies, R. A., Pardoen, J. A., Winkel, C., van den Berg, E. M., and Lugtenburg, J. (1985) Vibrational analysis of the all-trans retinal protonated Schiff base, *Biophys. J. 47*, 653−664.
42. Kandori, H., Shimono, K., Sudo, Y., Iwamoto, M., Shichida, Y., and Kamo, N. (2001) Structural changes of *pharaonis* phoborhodopsin upon photoisomerization of the retinal chromophore: Infrared spectral comparison with bacteriorhodopsin, *Biochemistry 40*, 9238−9246.
43. Furutani, Y., Iwamoto, M., Shimono, K., Kamo, N., and Kandori, H. (2002) FTIR spectroscopy of the M photointermediate in *pharaonis* rhoborhodopsin, *Biophys. J. 83*, 3482−3489.
44. Mathies, R., Freedman, T. B., and Stryer, L. (1977) Resonance Raman studies of the conformation of retinal in rhodopsin and isorhodopsin, *J. Mol. Biol. 109*, 367−372.
45. Palings, I., Pardoen, J. A., van den Berg, E., Winkel, C., Lugtenburg, J., and Mathies, R. A. (1987) Assignment of fingerprint vibrations in the resonance Raman spectra of rhodopsin, isorhodopsin, and bathorhodopsin: Implications for chromophore structure and environment, *Biochemistry 26*, 2544−2556.
46. Kandori, H., Kinoshita, N., Yamazaki, Y., Maeda, A., Shichida, Y., Needleman, R., Lanyi, J. K., Bizounok, M., Herzfeld, J., Raap, J., and Lugtenburg, J. (1999) Structural change of threonine 89 upon photoisomerization in bacteriorhodopsin as revealed by polarized FTIR spectroscopy, *Biochemistry 38*, 9676−9683.
47. Kandori, H., Yamazaki, Y., Shichida, Y., Raap, J., Lugtenburg, J., Belenky, M., and Herzfeld, J. (2001) Tight Asp-85−Thr-89 association during the pump switch of bacteriorhodopsin, *Proc. Natl. Acad. Sci. U.S.A. 98*, 1571−1576.

BI050219W